CONFOCAL MICROWAVE IMAGING FOR BREAST TUMOUR DETECTION: PRACTICAL FEASIBILITY

M. Okoniewski[(1)], D. Popovic[(2)], E.C. Fear[(3)], J. Sill[(4)] and M.A. Stuchly[(5)]

[(1)] Electrical and Computer Engineering, University of Calgary, 2500 University Drive NW, Calgary, AB, Canada T2N 14N email: michal@enel.ucalgary.ca
[(2)] As (1) above, but email: popovic@enel.ucalgary.ca
[(3)] As (1) above, but email: fear@enel.ucalgary.ca
[(4)] Electrical and Computer Engineering, University of Victoria, Box 3055, STN CSC, Victoria, BC, Canada V8W 3P6 email: jsill@engr.uvic.ca
[(5)] As (4) above, but email: mstuchly@engr.uvic.ca

ABSTRACT

Confocal Microwave Imaging (CMI) [1-4] is slowly progressing from the theoretical stage involving extensive simulations to experimental feasibility studies. Two aspects need to be addressed: (i) the practical capability of CMI to detect tissue abnormalities, and (ii) verification of the hypothesis that large contrast exists between electrical parameters of breast cancer and normal breast tissue. In this paper we present initial results on both aspects of the technology.

EXPERIMENTAL VERIFICATION OF CMI ALGORITHM

FDTD simulations have been performed to test the feasibility of detecting and localizing small tumours in 3D with CMI (e.g. [1-4]). Initial experimental verification is underway with a simple phantom consisting of a PVC pipe that contains a metallic or wooden sphere. The spheres represent tumours, while the pipe represents skin. While the electrical properties of these materials do not represent actual tissue properties, the contrasts between the materials are similar to the contrasts expected in tissues (e.g. air/PVC contrast is similar to breast tissue/skin). Experimental results have been reported for a configuration with the PVC pipe axis oriented parallel to the antenna. In this case, the pipe is rotated and illuminated by an antenna after each rotation. This creates a synthetic array in which the antennas encircle the pipe. Results demonstrated successful detection and localization of tumours [5]. The experiment reported here is designed to complement the previously reported experimental results. The experimental configuration consists of a PVC pipe, antenna and hemispherical tumour placed on a ground plane (Fig. 1). The PVC pipe is sliced in half parallel to the axis, and the cut-side is placed in contact with the ground plane. The antenna is placed 10 cm from the edge of the pipe and scanned parallel to the axis of the pipe in 2.5 cm increments. Data are acquired at 13 locations, creating a synthetic array. The sphere is placed inside of the pipe. Two cases are tested: a metal hemisphere with diameter of 2.7 cm and a wood hemisphere with diameter of 3.8 cm. The distances between the edge of the pipe and center of the sphere are 7.5 cm (metal) and 7.6 cm (wood). The metal sphere is at the center of the array, while the wood sphere is 7 cm off center. A resistively loaded monopole antenna illuminates the phantom, and reflections are recorded at the same antenna with an 8720C vector network analyzer (Agilent Technologies, Palo Alto, CA, USA).

The reflections recorded at the antennas are processed to form images with the following steps. First, the signals are transformed from the frequency to time domain. This involves weighting the spectrum of the measured data to synthesize a differentiated Gaussian pulse, then transforming the signals to the time domain with an inverse chirp-z transform [6]. Next, a calibration step is performed. The returns recorded with only an antenna present are subtracted from the total signal to reduce the incident pulse. The dominant reflections in the signal after calibration are due to the PVC pipe. To reduce these reflections, skin subtraction and gating are applied. The average of the reflections from the pipe recorded at each antenna is calculated and subtracted from each signal. The reflection from the second pipe interface is determined, and a time gate is applied to the signal to remove this response. This involves identifying the initial pipe reflection, and correlating this response to the calibrated signal. The second largest peak in the correlated signal is used to identify the reflection from the far side of the PVC pipe. All data beyond this point in the skin-subtracted signal are zero padded. Integration is applied to transform the midpoint (in

time) of the differentiated Gaussian signal from a zero to a maximum. This is necessary for coherent addition of the maxima of signals. Radial spreading compensation accounts for the 1/r decrease in amplitude of the wave with distance from its source. Finally, the image is formed by scanning the focus of the array through the region of interest, which is accomplished by appropriately time-shifting and summing signals, forms the image.

Images of a pipe containing metallic and wooden spheres are reconstructed. In both cases, the sphere is detected, localized and the response location is in reasonable agreement with the physical location of the sphere. Signal-to-clutter ratios compare the maximum tumour response to the maximum non-tumour response in the image. The S/C ratio for the metal sphere is 5.5 dB, while the wood sphere has an S/C ratio of 4.2 dB. As expected, the S/C ratio is smaller for the less strongly scattering object. The tumour response is well localized in the x direction (perpendicular to the array), and more extensive in the y direction (parallel to the array). In contrast, experiments with the PVC pipe oriented parallel to the antenna showed good localization in both x and y directions. Similar observations were made with simulated results: the tumour response is well localized when the antennas encircle the model; when antennas are scanned past the tumour, a less localized response is observed. The localization improves with a larger array span, implying a tradeoff between number of antennas required, data acquisition time, and image quality.

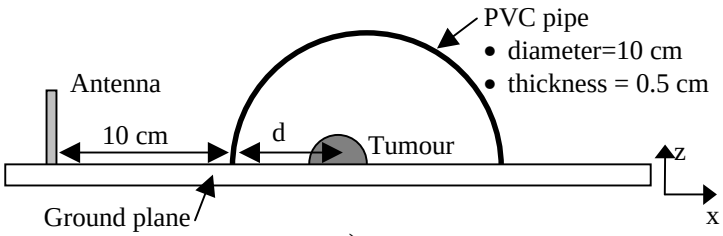

a)

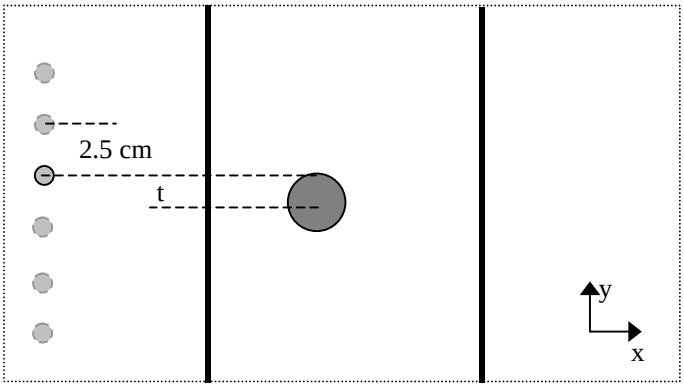

b)

Fig. 1 Experimental configuration a) The distance *d* is 7.5 cm for the metal tumour (diameter 2.7 cm) and 7.6 cm for the wood tumour (diameter 3.8 cm). b) For both experiments, data are acquired at 13 antenna locations. For the metal tumour, *t=0 cm*. With the wood tumour, *t=-7 cm*.

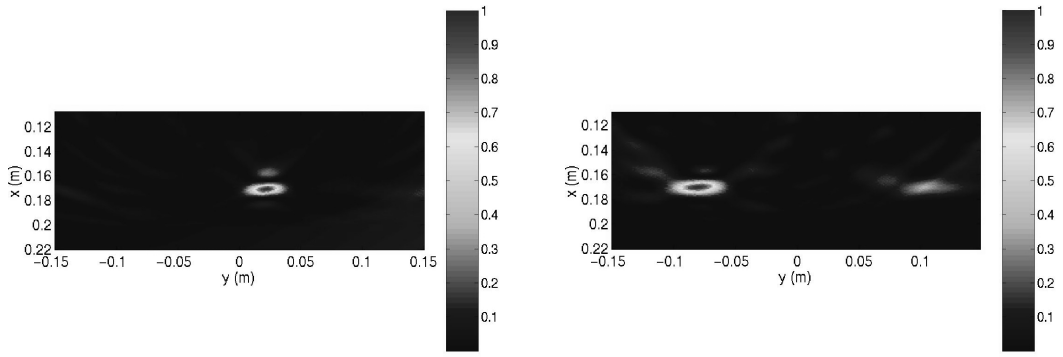

a) b)

Fig. 2 a) Image of metal sphere. b) Image of wood sphere.

EXPERIMENTAL EVALUATION OF DIELECTRIC SENSOR

The measurement technique used for the *in vivo* dielectric spectroscopy of breast tissue specimens relies on small-aperture open-ended coaxial probes, due to their broadband response and simplicity, and no need for extensive sample preparation. Complete characterization of the probe response and the quality of the contact with the specimen are critical to the reliability and accuracy of the measurements. Very high frequencies contained in the spectrum of interest (up to 20 GHz) and considerable variation in size of the breast tissue specimens prompted a pilot study into the volume sensing properties of these probes [7] to ensure the highest possible accuracy in the dielectric-properties estimates. The sensing volume depends mainly on the probe aperture, and is only slightly dependant on the liquid being measured. Field energy focuses close to the probe aperture, with penetration depth very weakly dependent on frequency.

During the extensive numerical and experimental analysis of simple probes made of sections of semi-rigid cable, it became clear that the small geometrical changes in the probe aperture region, arising e.g. from handling and inaccurate manufacturing, have profound effects on the observed reflection coefficient. The magnitude of the effect is related to the difference between the dielectric parameters of the tissue-equivalent liquid under test and probe dielectric. Teflon retracting into the probe, or bulging out, is one of more common imperfections observed under a microscope. This mechanical flaw can result from improper manufacturing, and/or differential thermal expansion. Even small inaccuracies of the order of 0.1 mm can lead to dramatic changes in the probe properties (Fig 3), manifested by errors as high as 25% for higher permittivity liquids at higher frequencies (15-20 GHz). Similar effects were observed for the cases when teflon covers metal conductors of the probe, which often occurs as a result of polishing of the probe end. Smaller errors (~7%) arise from liquid under test leaking into the spaces between the dielectric and inner/outer conductor, as the simple probes are not sealed.

The above results show the need for an improved probe design and superior manufacturing processes to minimize the possibility of geometrical imperfections at the aperture. A new probe has been built out of 3 sections of high quality coaxial cable using dielectrics whose thermal properties are similar to those of the metal and with 10μm flatness accuracy at the aperture. Borosilicate glass is used as the dielectric in the final section of the probe and is hermetically sealed to the metal conductors. The complex probe construction complicates measurement, particularly that standard calibration procedures cannot be used. However, accurate measurements of the probe shape have been made with the help of X-ray, and allowed for numerical generation of de-embedding S-matrix for the probe. This procedure yielded measurement results that are within 1-2% of the results obtained from simulations of an ideal homogeneous borosilicate probe. Previous results with semi-rigid teflon probes were within 15-20% of the theoretical values. This indicates that the new probes are suitable as sensors for high fidelity *in vivo* tissue measurements and characterization. It will be used in a switched, multi-probe measurement system for fast and accurate tissue measurements.

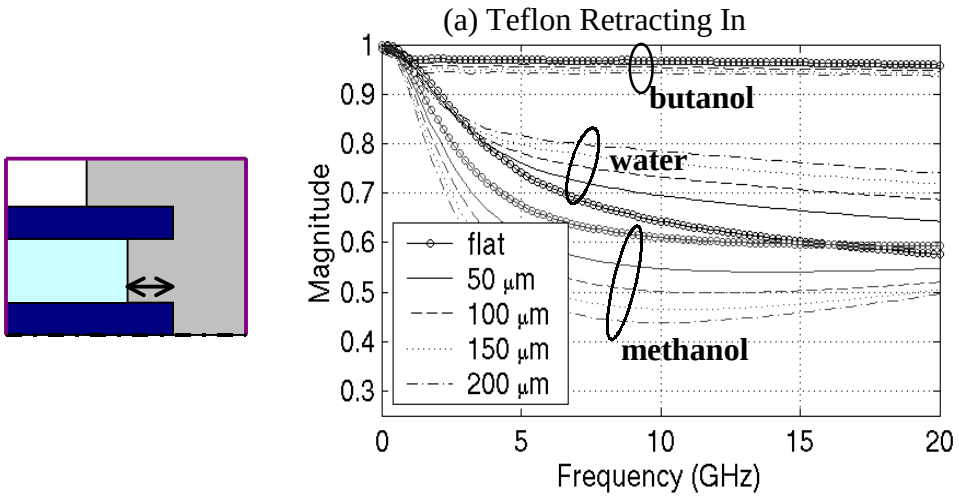

Fig 3. Effect of probe mechanical imperfections on reflection coefficient

CONCLUSIONS

Initial results obtained with simple phantoms indicate the possibility of detecting tumours. More work is required to improve localization of the tumour response along the axis of the phantoms, as well as to detect smaller objects. As results of tissue measurements with probes become available, this information will be used to build phantoms with more realistic material properties. Such phantoms allow closer comparison with database of computed results, as well as a more rigorous test of the feasibility of CMI for breast tumour detection.

REFERENCES

[1] S. C. Hagness, A. Taflove, and J. E. Bridges, "Two-dimensional FDTD analysis of a pulsed microwave confocal system for breast cancer detection: fixed-focus and antenna-array sensors," *IEEE Trans. Biomed. Eng.*, vol. 45, pp. 1470-1479, Dec. 1998.

[2] S. C. Hagness, A. Taflove, and J. E. Bridges, "Three-dimensional FDTD analysis of a pulsed microwave confocal system for breast cancer detection: design of an antenna-array element," *IEEE Trans. Antennas Propag.*, vol. 47, pp. 783-791, May 1999.

[3] X. Li and S.C. Hagness, "A confocal microwave imaging algorithm for breast cancer detection," *IEEE Microwave and Wireless Components Letters*, vol. 11, March 2001, pp. 130-132.

[4] E.C. Fear, X. Li, S.C. Hagness, M.A. Stuchly, "Confocal microwave imaging for breast cancer detection: Localization of tumours in three dimensions", to appear in *IEEE Transactions on Biomedical Engineering*, 2002.

[5] E.C. Fear, A. Low, J. Sill and M.A. Stuchly, "Microwave System for Breast Tumour Detection: Experimental Concept Evaluation," to be presented at the *2002 AP-S International Symposium and UNHC/URSI Radio Science Meeting*, San Antonio, TX, June 16-21, 2002**.**

[6] B. Ulriksson, "Conversion of frequency-domain data to the time domain," *Proc. IEEE,* vol. 74, Jan. 1986, pp. 74-77.

[7] D. Popovic, M. Okoniewski, D. Hagl, S.C. Hagness, J.Booske, "Volume sensing properties of open-ended coaxial probes for dielectric spectroscopy of breast tissue", *2001 IEEE International Antennas and Propagation Symposium*, vol. 1, 2001, pp. 250 –252.